Scilight

Applied Mathematics and Statistics
https://www.sciltp.com/journals/ams

Article

H_∞ Control of Markov Jump Reaction-Diffusion Neural Networks via a Dynamic Event-Triggered Mechansim with Actuator Faults

Yang Liu, Kui Ding *, Xiaotai Wu * and Ying Zhao

School of Mathematics-Physics and Finance, Anhui Polytechnic University, Wuhu 241000, China
* Correspondence: dingkui_2016@163.com (K.D.); aaxtwu@126.com (X.W.)

How To Cite: Liu, Y.; Ding, K.; Wu, X.; et al. H_∞ Control of Markov Jump Reaction-Diffusion Neural Networks via a Dynamic Event-Triggered Mechansim with Actuator Faults. *Applied Mathematics and Statistics* **2025**, *2*(2), 7. https://doi.org/10.53941/ams.2025.100007

Received: 2 November 2025
Revised: 28 November 2025
Accepted: 9 December 2025
Published: 15 December 2025

Abstract: This paper investigates the problem of H_∞ control of Markov jump reaction-diffusion neural networks (MJRDNNs) via a dynamic event-triggered mechanism with actuator faults. First, by introducing reaction-diffusion terms into neural networks with Markovian switching, a more applicable class is constructed. Considering the communication pressure of MJRDNNs, this paper adopts a dynamic event-triggered mechanism to make the model more practical. By introducing an internal dynamic variable, the event-triggered mechanism has a more flexible threshold. The potential actuator fault in each network node is also considered. Secondly, an integral feedback controller is presented to study the control problem and $\mathcal{H}_\infty$ performance of MJRDNNs. By constructing an integral-form Lyapunov-Krasovskii (L-K) functional, some sufficient conditions can be obtained. Moreover, by using matrix techniques, the sufficient conditions are transformed into solvable linear matrix inequalities (LMIs), and the controller gain can also be derived. Finally, a numerical example is presented to demonstrate the effectiveness of the results.

Keywords: markov jump reaction diffusion neural networks; dynamic event-triggered mechanism; actuator faults; H_∞ control

1. Introduction

Network networks (NNs) have exerted profound impacts in a range of areas, including industry, healthcare, and transportation, and the research on NNs has long been a prominent subject in the control domain over the past several decades [1–4]. In some practical models, diffusion phenomena will occur from time to time. Reaction-diffusion neural networks (RDNNs) can well describe this phenomenon through partial differential equations with reaction-diffusion terms. In recent years, researchers have achieved many fruitful results in the study of RDNNs [5–7]. For instance, the synchronization problem of RDNNs with random time-varying delays based on distributed measurements or boundary measurements has been studied in [5]. In [6], the unified control problem of synchronization for complex-valued interconnected NNs with Markovian jump parameters and nonlinear coupling protocols has been explored. In [7], the problem of data confusion caused by large transmission delays in semi-Markov RDNNs under the time-space sampled-data control strategy with multiple event-triggered protocols and multi-asynchronous mechanisms has been studied.

Markov processes can effectively describe the dynamic switching processes of systems [8–11]. When encountering unforeseen environmental disturbances or random failures of network components, the topological structure of network systems usually undergoes dynamic adjustments over time. In recent years, an increasing number of scholars have focused on the research of MJRDNNs. For instance, ref. [12] has focused on MJRDNNs and multiple disturbances, and a composite disturbance rejection control strategy based on a disturbance observer has been proposed. A synchronization control method for MJRDNNs based on a dynamic-memory event-triggered protocol has been studied in [13]. In [14], the input-to-state exponentially mean-square stability of stochastic MJRDNNs with parameter uncertainties and exogenous disturbances has been studied.

Actuator faults are a critical concern in control systems, when faults occur, such as partial failure or complete outage, the intended control objectives may not be achieved [15–17]. Therefore, addressing actuator faults and ensuring the robustness of control systems in their presence is of great practical significance, and numerous scholars have also conducted research on this topic. Specifically, in [18], the problem of asynchronous control for fuzzy hidden Markov jump systems with actuator faults has been researched. The study in [19] has investigated the stochastic finite-time boundedness and H_∞ performance of continuous-time semi-Markov jump systems with actuator faults. The problem of adaptive fault-tolerant compensation control for Markov jump systems with simultaneous additive and multiplicative actuator faults based on a fuzzy logic system has been examined in [20].

Due to the large number of network nodes and mode transitions in MJRDNNs, the burden on network communication will also be intensified. The introduction of an event-triggered mechanism can well reduce communication pressure, decrease communication bandwidth, and save communication resources. The event-triggered mechanism sets an event-triggered function to prevent unnecessary information from being transmitted [21]. Over the past decades, scholars have conducted research on different time-triggered mechanisms and achieved excellent results [22–27]. In [22], a dynamic variable has been introduced to make the threshold for event triggering change over time. Compared with the general event-triggered mechanism, the dynamic event-triggered mechanism has fewer triggering times, which is more conducive to saving network resources.

Based on the aforementioned, it is meaningful to study MJRDNNs with actuator faults under the event-triggered mechanism. However, existing results rarely involve this aspect. To fill this gap, this paper investigates the H_∞ control of MJRDNNs with actuator faults based on a dynamic event-triggered mechanism. The main contributions of this paper are summarized as follows:

(1) Different from the existing works [17,18], this paper focuses on the H_∞ performance of MJRDNNs with actuator faults under an event-triggered mechanism. The MJRDNNs in this paper are more suitable for complex models, which takes the multi-dimensional space, actuator faults into consideration. There are also a few works investigated the H_∞ performance at triggering instants, which is the focus of this paper.

(2) By introducing an internal dynamic variable expressed by a differential equation, the triggering threshold becomes more flexible and greatly reduces the number of triggering instants in event triggering. In addition, this paper adopts a discrete sampling-based event-triggered approach, which effectively avoids the Zeno phenomenon. Moreover, by utilizing the upper and lower bounds of actuator faults, the expected performance indices are achieved without knowing the specific fault data.

(3) Through the construction of a L-K functional, several sufficient conditions ensuring the stability are obtained, and the H_∞ performance for MJRDNNs is also derived. Subsequently, by matrix computations, these conditions are converted into a solvable convex optimization problem.

Notations : Throughout the paper, the p-dimensional Euclidean space is denoted by $\mathbb{R}^p$, the $p \times q$-dimensional real matrices is represented by $\mathbb{R}^{p\times q}$, $\mathbb{E}$ represents the expectation. For any matrix W, $W^\top$ represents the transpose of W, diag$\{W_1, \cdots, W_j\}$ stands for a block diagonal matrix, where $W_1, \cdots, W_j$ denote its diagonal elements respectively. Similarly, col$\{\cdot\}$ denotes a column vector. Let $\mathcal{L}_2(H)$ denotes a Hilbert space composed of square-integrable functions $\varsigma(\vartheta, t)$, where $\vartheta \in H \subset \mathbb{R}^n$, $\mathcal{H}^1(H)$ denotes the Sobolev space of absolutely continuous scalar function $\varsigma(\vartheta, t)$, the function $\varsigma(\vartheta, t)$ has absolutely continuous $\frac{\partial\varsigma(\vartheta,t)}{\partial\vartheta}$ and $\frac{\partial^2\varsigma(\vartheta,t)}{\partial\vartheta^2} \in \mathcal{L}_2(H)$, $\|\varsigma(\vartheta, t)\|_2$ is defined as $\left(\int_H \varsigma(\vartheta, t)^\top \varsigma(\vartheta, t)\right)^{1/2} d\vartheta$, $\overline{1, n}$ represents the set of positive integers $\{1, \cdots, n\}$.

2. Problem Formulation and Preliminaries

System Description

The structure for the control problem of MJRDNNs with a dynamic event-triggered mechanism is shown in Figure 1. Consider the following MJRDNNs described by

$$\begin{cases} \dfrac{\partial\varsigma(\vartheta,t)}{\partial t} = D_s \displaystyle\sum_{s=1}^{\overline{m}} \dfrac{\partial^2\varsigma(\vartheta,t)}{\partial\vartheta_s^2} - A_{r_t}\varsigma(\vartheta,t) \\ \qquad\qquad + B_{r_t} f(\varsigma(\vartheta,t)) + C_{r_t} u^F(\vartheta,t) + F_{r_t}\omega(\vartheta,t), \\ z(\vartheta,t) = G_{r_t}\varsigma(\vartheta,t), \end{cases} \tag{1}$$

where $\vartheta = (\vartheta_1, \cdots, \vartheta_{\overline{m}})^\top \in H \subset \mathbb{R}^{\overline{m}}$ represents the space variables; $\varsigma(\vartheta, t) = (\varsigma_1(\vartheta, t), \cdots, \varsigma_n(\vartheta, t))^\top \in \mathbb{R}^n$ is the neuron state vector with n nodes, in which $\varsigma_k(\vartheta, t)$ denotes the kth neuron at time t and in space ς, $k \in \overline{1, n}$; $f(\varsigma(\vartheta, t)) = (f(\varsigma_1(\vartheta, t)), \cdots, f(\varsigma_n(\vartheta, t)))^\top \in \mathbb{R}^n$ stands for the neuron activation function; $u^F(\vartheta, t) \in \mathbb{R}^{p_1}$,

$\omega(\vartheta,t) \in \mathbb{R}^{p_2}$, and $z(\vartheta,t) \in \mathbb{R}^{p_3}$ represent the control input with actuator faults, external disturbance and control output respectively; D_s, A_{r_t}, B_{r_t}, C_{r_t}, and F_{r_t} are known real matrices, in which $D_s = \textbf{diag}\{d_{1s}, \cdots, d_{ns}\} \in \mathbb{R}^{n\times n}$ represents the the transmission diffusion coeffiient; $A_{r_t} = \textbf{diag}\{a_{1r_t}, \cdots, a_{nr_t}\} \in \mathbb{R}^{n\times n}$; $B_{r_t} = [b_{pqr_t}]_{p,q\in\overline{1,n}} \in \mathbb{R}^{n\times n}$ denotes the connection weight matrix; $C_{r_t} \in \mathbb{R}^{n\times p_1}$, $F_{r_t} \in \mathbb{R}^{n\times p_2}$, and $G_{r_t} \in \mathbb{R}^{n\times p_3}$. For all $k \in \overline{1,n}$, consider the variables $\omega(\vartheta,t)$, d_{ksr_t}, and a_{kr_t}; it holds that $\omega(\vartheta,t) \in \mathcal{L}_2[0,\infty)$, $d_{ksr_t} > 0$, and $a_{kr_t} > 0$. $r(t)$ is Markov process which takes values in $\mathcal{N} = \overline{1,N}$, the transition probability is given by

$$\mathbb{P}(r(t+\epsilon) = i|r(t) = j) = \begin{cases} \kappa_{ij}\epsilon + o(\epsilon), & i \neq j, \\ 1 + \kappa_{ij}\epsilon + o(\epsilon), i = j, \end{cases} \tag{2}$$

where ϵ is the sojourn-time satisfying $\epsilon > 0$ and $\lim_{\epsilon\to 0} \frac{o(\epsilon)}{\epsilon} = 0$. κ_{ij} represents the transition rate satisfying $\kappa_{ij} = -\sum_{i=1,j\neq i}^{N} \kappa_{ij} < 0$. For simplicity, let $r(t) = i$.

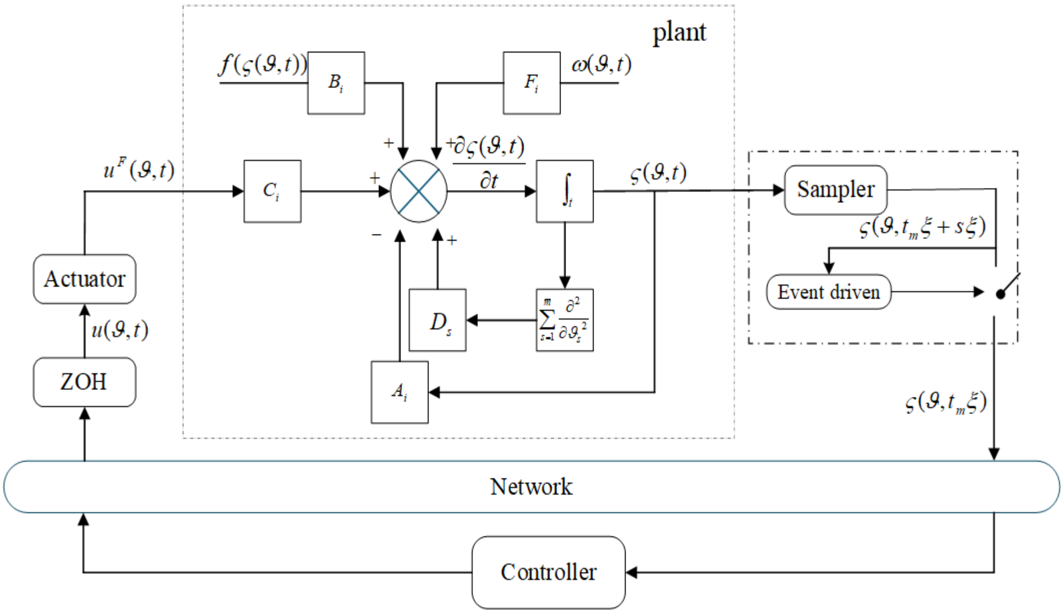

Figure 1. Structural block diagram of the system.

Typically, the following assumptions are made regarding the activation function $f(\cdot)$.

Assumption 1. *For any $k \in \overline{1,n}$ and scalars α, $\beta \in \mathbb{R}$, there holds*

$$0 \leq \frac{f_k(\alpha) - f_k(\beta)}{\alpha - \beta} \leq \theta_k, \tag{3}$$

where $f_k(\cdot)$ is the activation function satisfying $f_k(0) = 0$, θ_k is a positive constant satisfying $\theta_k > 0$.

Assumption 2. *For MJRDNNs (1), it satisfies the Dirichlet boundary conditions and initial conditions at $t = 0$ as follows*

$$\begin{aligned} &\varsigma(\vartheta,t) = 0, \quad (\vartheta,t) \in [0,\infty) \times \partial H \\ &\varsigma(\vartheta,t) = \varphi(\vartheta), \quad t = 0, \varsigma \in H \end{aligned} \tag{4}$$

in which ∂H represents the boundary of space H, $\varphi(\vartheta)$ is the continuous function of ϑ and takes bounded vector values.

Remark 1. *Dirichlet boundary conditions have quite a few advantages. On one hand, they can set clear and fixed values for the solution on the boundary, which is particularly useful for problems that require determining specific states or behaviors at the boundary. On the other hand, mathematical processing is simpler and more straightforward because it only involves the function itself without having to consider its derivatives. Moreover, it is well-suited for classic problems such as heat conduction and fluid mechanics, in which accurate boundary values can often be obtained through experiments or theoretical derivations.*

On the other hand, the actuator faults inevitably happen in the practical control systems. In this paper, $u^F(\vartheta,t)$ is used to denote the control signal from the actuator with actuator faults as follows:

$$u^F(\vartheta,t)=\delta u(\vartheta,t), \tag{5}$$

where $\delta=\textbf{diag}\{\delta_1,\cdots,\delta_{p_1}\}$, we assume that the condition holds for δ_k, $k\in\overline{1,p_1}$ as follows:

$$0\le\underline{\delta}_k\le\delta_k\le\overline{\delta}_k\le 1. \tag{6}$$

Remark 2. *The actuator fault function is a mathematical model that describes the relationship between actuator faults, input signals, and output responses, and can quantify the fault severity. Based on the aforementioned model, δ_k has upper and lower bounds $\overline{\delta}_k$ and $\underline{\delta}_k$, where δ_k represents the actuator of the ith node. When $\underline{\delta}_k=\overline{\delta}_k=1$, and the actuator is free from faults; when $0<\underline{\delta}_k<\delta_k<\overline{\delta}_k<1$, the actuator suffers a partial fault; when $\underline{\delta}_k=\overline{\delta}_k=0$, the actuator experiences a complete fault.*

For simplicity, let $\overline{\delta}=\textbf{diag}\{\overline{\delta}_1,\cdots,\overline{\delta}_{p_1}\}$, $\underline{\delta}=\textbf{diag}\{\underline{\delta}_1,\cdots,\underline{\delta}_{p_1}\}$, $\delta_b=\frac{\overline{\delta}+\underline{\delta}}{2}$, and $\delta_a=\frac{\overline{\delta}-\underline{\delta}}{2}$. It easily yield that

$$\delta_a\le\delta\le\delta_b. \tag{7}$$

The event-triggered mechanism is excellent for maintaining communication bandwidth and conserving communication resources. In this paper, $\{t_m\xi|t_m\in\mathbb{R}\}$ represents transmitted instants, ξ is the constant period, t_m represents the mth transmission. $\varsigma(\vartheta,t_m\xi)$ denotes the latest transmitted measurement, $\varsigma(\vartheta,t_m\xi+s\xi)$ denotes the current sampled data, and the following dynamic event-triggered mechanism is adopted:

$$\begin{aligned} t_{m+1}\xi=t_m\xi+\inf_{m\ge1}\big\{s\xi|\mu(\vartheta,t)+&\varepsilon(\sigma\varsigma^\top(\vartheta,t_m\xi)\Omega_1\varsigma(\vartheta,t_m\xi)\\ &-e_m^\top(\vartheta,t)\Omega_2e_m(\vartheta,t))<0\big\},\end{aligned} \tag{8}$$

in which $\sigma\in[0,1)$, $\varepsilon>0$, $e_m(\vartheta,t)=\textbf{diag}\{e_{m,1}(\vartheta,t),\cdots,e_{m,n}(\vartheta,t)\}$, where $e_{m,k}(\vartheta,t)=\varsigma_k(\vartheta,t_m\xi)-\varsigma_k(\vartheta,t_m\xi+s\xi)$, $k=1,\cdots,n$. Ω_1, Ω_2 are positive matrices which need to be solved, $\mu(\vartheta,t)>0$ denotes the dynamic variable that holds

$$\begin{aligned}\dot{\mu}(\vartheta,t)=&-\lambda\mu(\vartheta,t)+\sigma\varsigma^\top(t_m\xi)\Omega_1\varsigma(\vartheta,t_m\xi)\\ &-e_m^\top(\vartheta,t)\Omega_2e_m(\vartheta,t).\end{aligned} \tag{9}$$

The delay between sample instant and controller state is τ_{t_m}, interval $[t_m\xi+\tau_{t_m},t_{m+1}\xi+\tau_{t_{m+1}}]$ can be divided into $\cup_{s=0}^{d}\Upsilon(s,m)$, where $\Upsilon(s,m)=[t_m\xi+s\xi+\tau_{t_m+s},t_{m+1}\xi+(s+1)\xi+\tau_{t_{m+1+s}}]$ with $s=1,\cdots,q$ and $q=t_{m+1}-t_m-1$. Defining $\gamma_t=t-t_m\xi-s\xi$ for $t\in[t_m\xi+\tau_{t_m},t_{m+1}\xi+\tau_{t_{m+1}}]\triangleq\Upsilon$ the transmitted state can be expressed as

$$\varsigma(\vartheta,t_m\xi)=\varsigma(\vartheta,t-\gamma_t)+e_m(\vartheta,t), \tag{10}$$

where $t\in\Upsilon$.

Remark 3. *For continuous networked systems, it is difficult to measure the system states at every moment. This not only imposes extremely high requirements on components but also causes significant communication pressure, leading to the waste of a large amount of communication resources. By designing an event-triggered function, the event-triggered mechanism stops transmitting data with minor changes, thereby greatly reducing communication pressure. The dynamic event-triggered mechanism adopted in this paper introduces an internal dynamic variable into the original event-triggered function, making the threshold for event triggering more flexible.*

Remark 4. *The Zeno phenomenon is a necessary topic of discussion in event-triggered mechanisms; it refers to the occurrence of an infinite number of triggers within a finite time period. To avoid the Zeno phenomenon, this paper adopts an event-triggered mechanism in the form of discrete sampling. Since there exists a minimum lower bound for its sampling interval, the Zeno phenomenon will not occur.*

Lemma 1. *(See [26]) The following relation holds*

$$\dot{\gamma}(\vartheta,t)=1,\quad 0\le\tau_{t_m}\le\gamma_t\le(t_{m+1}-t_m)\xi+\tau_{t_{\xi+1}}$$

and there exists a constant γ_M that satisfies $\gamma_M\ge\gamma_t$.

Based on the analysis mentioned above, the dynamic event-triggered controller is chosen as follows:

$$u(\vartheta,t)=K_i\varsigma(\vartheta,t_m\xi), \tag{11}$$

which can be written as

$$u(\vartheta,t)=K_i(\varsigma(\vartheta,t-\gamma_t)+e_m(\vartheta,t)). \tag{12}$$

Substituting (5) and (12) into system (1), the system can be rewritten as follows

$$\begin{cases}\dfrac{\partial\varsigma(\vartheta,t)}{\partial t}=D_s\displaystyle\sum_{s=1}^{\overline{m}}\frac{\partial^2\varsigma(\vartheta,t)}{\partial\vartheta_s^2}-A_i\varsigma(\vartheta,t)\\ \qquad\qquad+B_if(\varsigma(\vartheta,t))+F_i\omega(\vartheta,t)\\ \qquad\qquad+C_i\delta K_i(\varsigma(\vartheta,t-\gamma_t)+e_m(\vartheta,t)),\\ z(\vartheta,t)=G_{r_t}\varsigma(\vartheta,t),\end{cases} \tag{13}$$

in which $t\in\Upsilon$.

Lemma 2. *(See [9]) For any matrices $U,V\in\mathbb{R}^{p\times q}$, there exist matrix W with appropriate dimensions, such that the following inequality holds*

$$U^\top V+V^\top U\le U^\top W^{-1}U+V^\top WV.$$

Lemma 3. *(See [12])For the given space H, and the state $\varsigma(\vartheta,t)$ is defined in system (13), where $\varsigma(\vartheta,t)=\psi(\vartheta_1,\cdots,\vartheta_{\overline{m}},t)\in C^1(H)$ and $\varsigma(\vartheta,t)|_{\partial_H}=0$, $C^1(H)$ represents the continuous function on the space H, ∂_H is the bound of H, there holds*

$$\int_H\varsigma(\vartheta,t)\frac{\partial^2\varsigma(\vartheta,t)}{\partial\vartheta_s^2}\mathrm{d}\vartheta\le-\frac{\pi^2}{4h_s^2}\int_H\varsigma(\vartheta,t)^2\mathrm{d}\vartheta, \tag{14}$$

where $|\vartheta_s|<h_s$ ($s=1,2,\ldots,\overline{m}$).

For convenience, let $\|x\|_2=\left(\int_H x^\top x\right)^{1/2}d\vartheta$, where $x\in\mathbb{R}^n$. Then, one has the following definition:

Definition 1. *(See [13]) The system (13) with $\omega(\vartheta,t)\equiv0$ is said to be stochastically stable for the initial condition and the boundary condition which has been defined in (4), if the following inequality holds*

$$\lim_{t^*\to\infty}\left\{\int_0^{t^*}\mathbb{E}\|\varsigma(\vartheta,t)\|_2^2\mathrm{d}t\right\}<\infty. \tag{15}$$

Definition 2. *(See [12]) For any $\omega(\vartheta,t)\in\mathcal{L}_2[0,\infty)$, two scalars $\beta>0$, $t^*\ge0$, the MJRDNNs (13) is said to be H_∞ with β index, if system (13) is stochastically stable and the following inequality under the zero initial condition holds:*

$$\mathbb{E}\left\{\int_0^{t^*}\|z(\vartheta,t)\|_2^2-\beta^2\|\omega(\vartheta,t)\|_2^2dt\right\}\le0. \tag{16}$$

3. Mian Results

In this section, the stochastic admissibility and H_∞ performance of system (13) will be considered.

Theorem 1. *Given parameters $\beta,\theta_k,\delta_k,\sigma,t^*$, if there exist positive definite symmetric matrices P_i, R, S, Ω_1, and Ω_2 such that the following condition holds*

$$\Xi=\begin{bmatrix}\Xi_1 & \Xi_2\\ * & -\beta^2I\end{bmatrix}<0, \tag{17}$$

where

$$\Xi_1=\begin{bmatrix}\Xi_{11} & P_iC_i\delta K_i & P_iC_i\delta K_i\\ * & -S+\sigma\Omega_1 & 0\\ * & * & \sigma\Omega_1-\Omega_2\end{bmatrix},\quad \Xi_2^\top=\begin{bmatrix}G_i & 0 & 0\end{bmatrix},$$

$$
\begin{aligned}
\Xi_{11} = & -\sum_{s=1}^{\overline{m}} \frac{\pi^2}{4h_s^2}(P_iD_s + D_s^\top P_i) + P_iA_i + A_i^\top P_i + P_iB_i \\
& \times B_i^\top P_i + L_b + R + \sum_{j=1}^{N} \kappa_{ij}P_j, \\
L_b = & \, \mathbf{diag}\{\theta_1, \cdots, \theta_n\}.
\end{aligned}
$$

The MJRDNNs (13) is said to be stochastically stable and satisfies the H_∞ performance with β index.

Proof. Consider the following L-K functional

$$
\begin{aligned}
V(\vartheta, t) = & \int_H \varsigma^\top(\vartheta, t)P_i\varsigma(\vartheta, t) + (\gamma_M - \gamma_t)\varsigma^\top(\vartheta, t-\gamma_t) \\
& \times S\varsigma(\vartheta, t-\gamma_t)\mathrm{d}\vartheta + \int_H \int_{t-\gamma_t}^{t} \varsigma^\top(\vartheta, t)R\varsigma(\vartheta, t)\mathrm{d}t\mathrm{d}\vartheta.
\end{aligned} \tag{18}
$$

The infinitesimal operator $\mathcal{L}$ corresponding to the L-K functional is introduced by

$$
\begin{aligned}
\mathcal{L}V(\vartheta, t) = & \lim_{\epsilon\to 0} \frac{1}{\epsilon}\Big\{\mathbb{E}\big\{V(r(t+\epsilon), \vartheta, t+\epsilon) \\
& |r(t) = i, \vartheta, t\big\} - V(i, \vartheta, t)\Big\},
\end{aligned}
$$

it can be obtained that

$$
\begin{aligned}
\mathcal{L}V(\vartheta, t) = & \int_H 2\varsigma^\top(\vartheta, t)P_i\Big[D_s\sum_{s=1}^{\overline{m}} \frac{\partial^2\varsigma(\vartheta, t)}{\partial\vartheta_s^2} - A_i\varsigma(\vartheta, t) \\
& + C_i\delta K_i(\varsigma(\vartheta, t-\gamma_t) + e_m(\vartheta, t)) + B_if(\varsigma(\vartheta, t)) \\
& + F_i\omega(\vartheta, t)\Big] + \varsigma^\top(\vartheta, t)\sum_{j=1}^{N} \kappa_{ij}P_j\varsigma(\vartheta, t)\mathrm{d}\vartheta \\
& + \int_H \varsigma^\top(\vartheta, t)R\varsigma(\vartheta, t)\mathrm{d}\vartheta - \int_H \varsigma^\top(\vartheta, t-\gamma_t) \\
& \times S\varsigma(\vartheta, t-\gamma_t)\mathrm{d}\vartheta.
\end{aligned} \tag{19}
$$

According to Lemma 1, there holds

$$
\begin{aligned}
& 2\int_H \varsigma^\top(\vartheta, t)P_iD_s\sum_{s=1}^{\overline{m}} \frac{\partial^2\varsigma(\vartheta, t)}{\partial\vartheta_s^2}\mathrm{d}\vartheta \\
& \leq -\sum_{s=1}^{\overline{m}} \frac{\pi^2}{4h_s^2}\int_H \varsigma^\top(\vartheta, t)(P_iD_s + D_s^\top P_i)\varsigma(\vartheta, t)\mathrm{d}\vartheta.
\end{aligned} \tag{20}
$$

By using Lemma 2, the following inequality can be obtained

$$
\begin{aligned}
& 2\varsigma^\top(\vartheta, t)P_iB_if(\varsigma(\vartheta, t)) \\
& \leq \varsigma^\top(\vartheta, t)P_iB_iB_i^\top P_i\varsigma(\vartheta, t) + f^\top(\varsigma(\vartheta, t))f(\varsigma(\vartheta, t)),
\end{aligned} \tag{21}
$$

since the activation function satisfying Assumption 1, set $\alpha = \varsigma(\vartheta, t)$, $\beta = 0$, one has

$$
f_k(\varsigma(\vartheta, t)) \leq \theta_k, \quad k = 1, \cdots, n \tag{22}
$$

thus

$$
f^\top(\varsigma(\vartheta, t))f(\varsigma(\vartheta, t)) \leq \varsigma^\top(\vartheta, t)L_b\varsigma(\vartheta, t), \tag{23}
$$

in which $L_b = \mathbf{diag}\{\theta_1, \cdots, \theta_n\}$.

Substituting (20), (21) and (23) into (19), there holds

$$\begin{aligned}\mathcal{L}V(\vartheta,t)\leq&-\sum_{s=1}^{\overline{m}}\frac{\pi^2}{4h_s^2}\int_H\varsigma^\top(\vartheta,t)(P_iD_s+D_s^\top P_i)\varsigma(\vartheta,t)\mathrm{d}\vartheta\\&+\int_H\varsigma^\top(\vartheta,t)(P_iA_i+A_i^\top P_i+P_iB_iB_i^\top P_i+L_b\\&+R+\sum_{j=1}^{N}\kappa_{ij}P_j)2\varsigma(\vartheta,t)+\varsigma^\top(\vartheta,t)P_iC_i\delta K_i\\&\times\varsigma(\vartheta,t-\gamma_t)+2\varsigma^\top(\vartheta,t)P_iC_i\delta K_ie_m(\vartheta,t)\\&+2\varsigma^\top(\vartheta,t)F_i\omega(\vartheta,t)-\varsigma^\top(\vartheta,t-\gamma_t)S\varsigma(\vartheta,t-\gamma_t)\\&-\lambda\mu(\vartheta,t)+\delta\varsigma^\top(\vartheta,t-\gamma_t)\Omega_1\varsigma(\vartheta,t-\gamma_t)\\&+2\varsigma^\top(\vartheta,t-\gamma_t)\delta\Omega_1e_m(\vartheta,t)+e_m^\top(\vartheta,t)(\delta\Omega_1-\Omega_2)\\&\times e_m(\vartheta,t)\mathrm{d}\vartheta,\end{aligned}\tag{24}$$

when $\omega(\vartheta,t)=0$, it can be obtained that

$$\mathcal{L}V(\vartheta,t)\leq\int_H\xi_1^\top(\vartheta,t)\Xi_1\xi_1(\vartheta,t)\mathrm{d}\vartheta,\tag{25}$$

where $\xi_1(\vartheta,t)=\mathbf{col}\{\varsigma(\vartheta,t)\ \ \varsigma(\vartheta,t-\gamma_t)\ \ e_m(\vartheta,t)\}$. Integrate both sides of (25) from 0 to t^* and then take the expectation of the result, one has

$$\begin{aligned}\mathbb{E}\left\{\int_0^{t^*}\mathcal{L}V(\vartheta,t)\mathrm{d}t\right\}&\leq-\lambda_{min}(\Xi_1)\mathbb{E}\left\{\int_0^{t^*}\|\xi_1(\vartheta,t)\|_2^2\mathrm{d}t\right\}\\&\leq-\lambda_{min}(\Xi_1)\mathbb{E}\left\{\int_0^{t^*}\|\varsigma(\vartheta,t)\|_2^2\mathrm{d}t\right\},\end{aligned}\tag{26}$$

in which $-\lambda_{min}(\Xi_1)$ denotes the smallest eigenvalue of matrix Ξ_1. By using Dynkin's formula, it can be obtained that

$$\mathbb{E}\{V(\vartheta,t^*)\}-\mathbb{E}\{V(\vartheta,0)\}\leq-\lambda\mathbb{E}\left\{\int_0^{t^*}\|\varsigma(\vartheta,t)\|_2^2\mathrm{d}t\right\},\tag{27}$$

Then, we can obtain that

$$\lim_{t^*\to\infty}\mathbb{E}\left\{\int_0^{t^*}\|\varsigma(\vartheta,t)\|_2^2\right\}\mathrm{d}t<\infty.\tag{28}$$

The stochastic stability of system (13) can be proved.

Next, the H_∞ performance with the β index of system (13) will be proved. Construct the following function

$$\mathcal{J}=\mathcal{L}V(\vartheta,t)+\|z(\vartheta,t)\|_2^2-\beta^2\|\omega(\vartheta,t)\|_2^2.\tag{29}$$

By system (13), there holds $\|z(\vartheta,t)\|_2^2=\int_H\varsigma^\top(\vartheta,t)G_i^\top G_i\,\varsigma(\vartheta,t)d\vartheta$. Then, by using Schur complement, one has

$$\mathcal{J}\leq\int_H\xi_2^\top(\vartheta,t)\Xi\xi_2(\vartheta,t)\mathrm{d}\vartheta,\tag{30}$$

where $\xi_2(\vartheta,t)=\mathbf{col}\{\varsigma(\vartheta,t)\ \ \varsigma(\vartheta,t-\gamma_t)\,e_m(\vartheta,t)\ \omega(\vartheta,t)\}$.

By using the similar way to (25), there holds

$$\mathbb{E}\left\{\int_0^{t^*}\mathcal{J}\mathrm{d}t\right\}<0.\tag{31}$$

Under the zero initial condition, it can be shown that

$$\mathbb{E}\left\{\int_0^{t^*}\|z(\vartheta,t)\|_2^2-\beta^2\|\omega(\vartheta,t)\|_2^2\mathrm{d}t\right\}\leq-\mathbb{E}\{V(t^*)\},\tag{32}$$

due to $V(\vartheta, t) \geq 0$, one can obtain that

$$\mathbb{E}\left\{\int_0^{t^*} \|z(\vartheta,t)\|_2^2 - \beta^2\|\omega(\vartheta,t)\|_2^2 \mathrm{d}t\right\} \leq 0, \tag{33}$$

the H_∞ performance with the β-index of system (13) can be obtained. The proof is completed. □

Theorem 1 has given the sufficient condition to prove the stochastic stability and the H_∞ performance with the β index of MJRDNNs (13). The following theorem converts these conditions into a linear matrix inequality problem solvable by MATLAB.

Theorem 2. *Given parameters $\beta, \theta_i, \delta_i, \sigma, T$, if there exist positive define symmetric matrices V_i, $\widetilde{R}$, $\widetilde{S}$, $\widetilde{\Omega}_1$, $\widetilde{\Omega}_2$ such that the following condition holds*

$$\Lambda = \begin{bmatrix} \Lambda_1 & \Lambda_2 \\ * & \Lambda_4 \end{bmatrix} < 0, \tag{34}$$

where

$$\begin{aligned}
\Lambda_1 &= \begin{bmatrix} \Lambda_{11} & C_i\delta W_i & C_i\delta W_i & F_i & V_i\sqrt{L_b} \\ * & -\widetilde{S}+\sigma\widetilde{\Omega}_1 & \sigma\widetilde{\Omega}_1 & 0 & 0 \\ * & * & \sigma\widetilde{\Omega}_1-\widetilde{\Omega}_2 & 0 & 0 \\ * & * & * & -\beta^2 I & 0 \\ * & * & * & * & -I \end{bmatrix}, \\
\Lambda_2^\top &= \begin{bmatrix} \Lambda_{21} & 0 & 0 & 0 & 0 \end{bmatrix}, \\
\Lambda_4 &= \mathbf{diag}\{-V_1, \cdots, -V_{i-1}, -V_{i+1}, \cdots, -V_M\}, \\
\Lambda_{11} &= -\sum_{s=1}^{\overline{m}} \frac{\pi^2}{4h_s^2}(V_iD_s + D_s^\top V_i) + A_iV_i + V_iA_i^\top + B_iB_i^\top \\
&\quad + \widetilde{R} + \kappa_{ii}V_i, \\
\Lambda_{21} &= \mathbf{col}\{\sqrt{\kappa_{i1}}V_1, \cdots, \sqrt{\kappa_{i(i-1)}}V_i, \sqrt{\kappa_{i(i+1)}}V_i, \cdots, \sqrt{\kappa_{in}}V_i\}, \\
\widetilde{R} &= V_i^\top RV_i,\ \widetilde{S} = V_i^\top SV_i,\ \widetilde{\Omega}_1 = V_i^\top\Omega_1V_i,\ \widetilde{\Omega}_1 = V_i^\top\Omega_1V_i.
\end{aligned}$$

the controller gain is expressed as $K_i = W_iV_i^{-1}$, where $V_i = P_i^{-1}$. Then, the system (13) is stochastically stable and the H_∞ performance of system (13) with β index can be achieved.

Proof. By schur complement, (34) can be rewritten as

$$\overline{\Lambda} = \begin{bmatrix} \overline{\Lambda}_{11} & C_i\delta W_i & C_i\delta W_i & F_i \\ * & -\widetilde{S}+\sigma\widetilde{\Omega}_1 & \sigma\widetilde{\Omega}_1 & 0 \\ * & * & \sigma\widetilde{\Omega}_1-\widetilde{\Omega}_2 & 0 \\ * & * & * & -\beta^2 I \end{bmatrix} < 0, \tag{35}$$

where

$$\begin{aligned}
\overline{\Lambda}_{11} &= \sum_{s=1}^{\overline{m}} \frac{\pi^2}{4h_s^2}(V_iD_s + D_s^\top V_i) + A_iV_i + V_iA_i^\top + B_iB_i^\top \\
&\quad + \widetilde{R} + V_iL_bV_i + \sum_{i=1}^{N} \kappa_{ij}V_j.
\end{aligned}$$

Set $\zeta = \mathbf{diag}\{V_i, V_i, V_i, I\}$, pre- and post multiplying (17) with $\zeta^\top$ and ζ, we can obtain that (35) holds. The proof is complement. □

4. Simulation

Consider the MJRDNNs as follows:

$$\begin{cases} \frac{\partial\varsigma(\vartheta,t)}{\partial t} = D_s \sum_{k=1}^{M} \frac{\partial^2 \varsigma(\vartheta,t)}{\partial m_k^2} - A_i\varsigma(\vartheta,t) \\ \qquad + C_i\alpha K_i(\varsigma(\vartheta,t-\gamma_t) + e_m(\vartheta,t)) \\ \qquad + B_i f(\varsigma(\vartheta,t)) + F_i\omega(\vartheta,t), \\ \\ z(\vartheta,t) = G_i\varsigma(\vartheta,t), \end{cases} \tag{36}$$

in which

$$\begin{aligned} &D_s = \textbf{diag}\{0.01, 0.2\}, \\ &A_1 = \textbf{diag}\{1.3, 1.1\}, \quad A_2 = \textbf{diag}\{0.2, 0.9\}, \\ &B_1 = \begin{bmatrix} 0.4 & 0 \\ 0 & 0.4 \end{bmatrix}, \quad B_2 = \begin{bmatrix} 0.5 & 0 \\ 0 & 1 \end{bmatrix}, \\ &C_1 = \begin{bmatrix} 1.5 & 0.9 \end{bmatrix}^\top, \quad C_2 = \begin{bmatrix} 1.4 & 0.8 \end{bmatrix}^\top, \\ &F_1 = \begin{bmatrix} 0.12 & 0.12 \end{bmatrix}^\top, \quad F_2 = \begin{bmatrix} 0.1 & 0.1 \end{bmatrix}^\top, \\ &G_1 = \begin{bmatrix} 0.3 & 0.2 \end{bmatrix}, \quad G_2 = \begin{bmatrix} 0.5 & 0.1 \end{bmatrix}. \end{aligned}$$

The other system parameters are defined as follows: $\delta = d_1\delta_a + d_2\delta_b$, where $d_1 + d_2 = 1$, $\delta_a = \textbf{diag}\{0.4, 0.2\}$, $\delta_b = \textbf{diag}\{0.6, 0.8\}$, $d_1 = 0.5$, $d_2 = 0.5$. $L_b = \textbf{diag}\{1.8, 1.6\}$, $\vartheta \in H = \{-0.5 < \vartheta < 0.5\}$, $\sigma = 0.3$, $\lambda = 0.01$, $f_i(\varsigma(\vartheta,t)) = tanh(\varsigma(\vartheta,t))$, the initial conditions $\varphi(\vartheta) = (0.4cos(2\pi\vartheta), 0.6cos(2\pi m))^\top$, the external disturbance $\omega = 0.6cos(\pi\vartheta)/(1+t^2)$, the transition rate of MJRDNNs is given by

$$\Pi = \begin{bmatrix} -4.5 & 4.5 \\ 3.6 & -3.6 \end{bmatrix},$$

and the change of models is shown in Figure 2b. Using the LMI Toolbox in MATLAB, the controller gain and matrices related to the event-triggered mechanism can be obtained, where

$$\begin{aligned} &K_1 = \begin{bmatrix} -0.2181 & -0.0006 \end{bmatrix}, \quad K_2 = \begin{bmatrix} -1.1028 & -0.0399 \end{bmatrix}, \\ &\Omega_1 = \begin{bmatrix} 6.3587 & -0.1765 \\ -0.1765 & 0.6138 \end{bmatrix}, \quad \Omega_2 = \begin{bmatrix} 7.4634 & 0.0993 \\ 0.0993 & 0.7225 \end{bmatrix}, \end{aligned}$$

and the H_∞ performance index is $\beta = 0.7769$.

By using the solved results to conduct simulation verification on system (36), it can be observed that system (36) is a MJRDNNs in one-dimensional space with two nodes and two modes. Figure 3a,b respectively show the state trajectories of the two nodes without control input in space H. Figure 3c,d respectively show the state trajectories of the two nodes under control input.

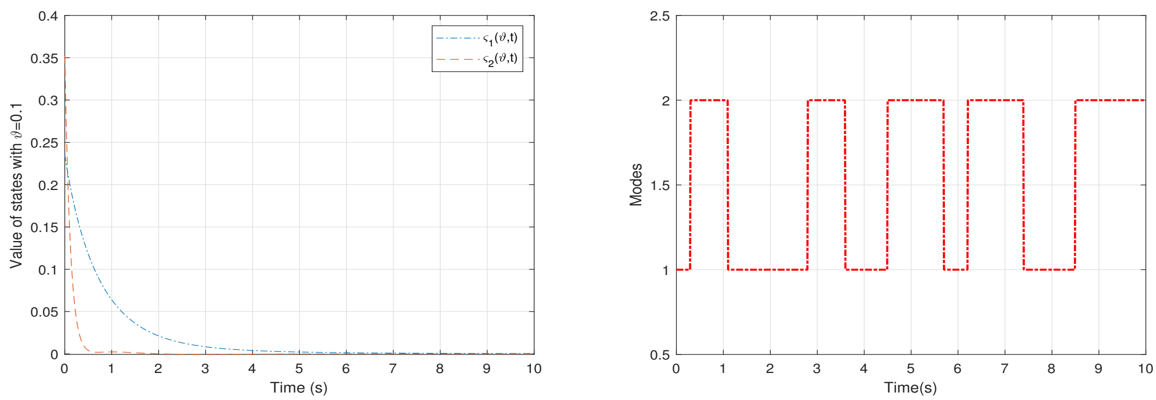

(a) **(b)**

Figure 2. (**a**) The evolution of states with $\vartheta = 0.1$; (**b**) Modal changes in the Markov process.

To better observe the state transition, $\vartheta = 0.1$ is selected, and the diagram of its plane variation is shown in Figure 2a.

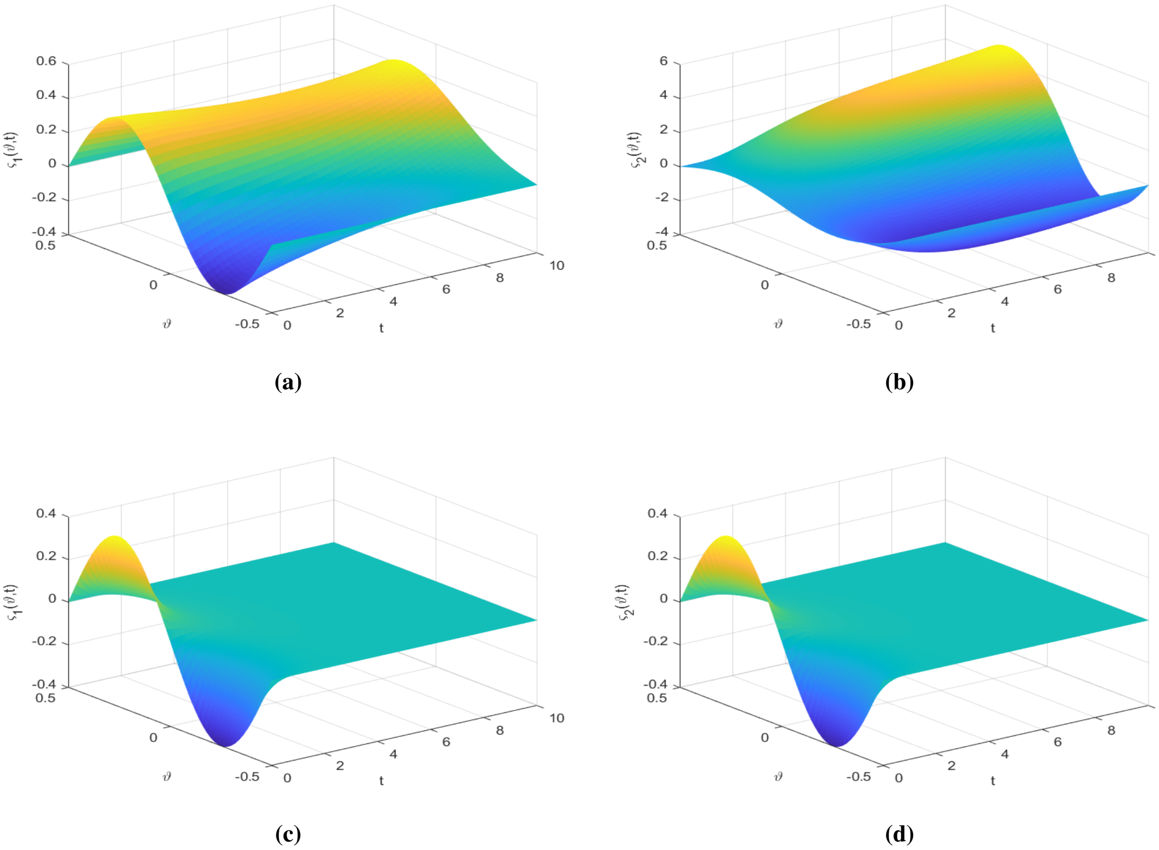

Figure 3. (**a**) The evolution of $\varsigma_1(\vartheta, t)$ in 0–10 s (open-loop); (**b**) The evolution of $\varsigma_2(\vartheta, t)$ in 0–10 s (open-loop); (**c**) The evolution of $\varsigma_1(\vartheta, t)$ in 0–10 s (close-loop); (**d**) The evolution of $\varsigma_2(\vartheta, t)$ in 0–10 s (close-loop).

Figure 4a,b respectively represent the triggering instants under the dynamic event-triggered mechanism and the static event-triggered mechanism.

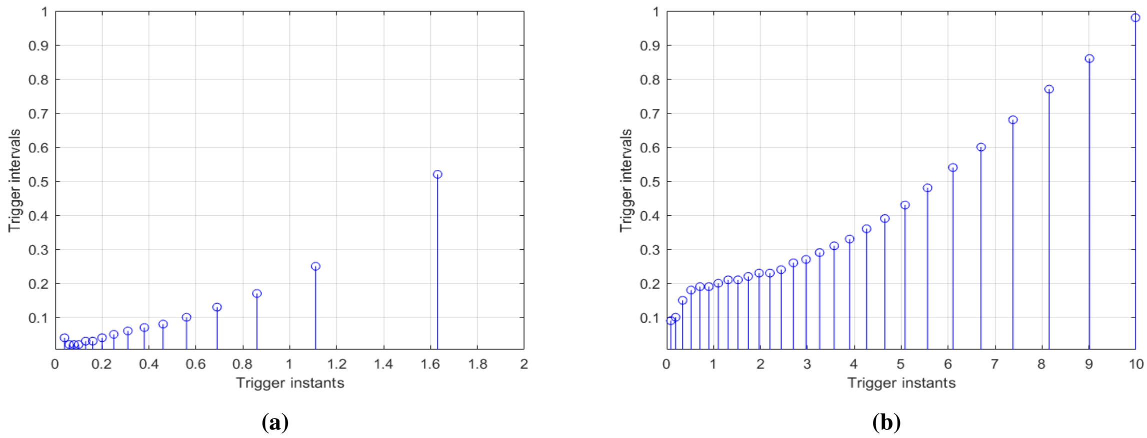

Figure 4. (**a**) Triggering instants of dynamic event-triggered mechanism; (**b**) Triggering instants of static event-triggered mechanism.

Obviously, the dynamic event-triggered mechanism has fewer triggering instances and can save more communication resources. From the perspective of system states, the system tends to be stable at around 2 s, and continuous triggering is not required. Therefore, the dynamic event-triggered mechanism is more suitable for system modeling.

5. Conclusions

This paper has investigated the H_∞ control of MJRDNNs with actuator faults under a dynamic event-triggered mechanism. Due to the presence of a large number of nodes and modal transitions in MJRDNNs, actuator faults and an event-triggered mechanism have been introduced in this paper for model establishment to improve system performance. To avoid the Zeno phenomenon, a discrete dynamic event-triggered mechanism has been designed in this paper, along with a corresponding controller. Subsequently, by constructing an integral-type L-K functional, sufficient conditions for the system to meet the performance indices have been proposed, which have been transformed into an LMI problem using matrix techniques. Finally, the effectiveness of the results has been verified through a numerical example. However, in practical systems, event triggering imposes extremely high requirements on components such as controllers and observers. In the future, we will focus on the stability and synchronization issues of reaction-diffusion systems under hybrid control methods.

Author Contributions

Y.L.: conceptualization, methodology, software; Y.L.: data curation, writing—original draft preparation; K.D.: visualization, investigation; X.W.: supervision; Y.Z.: software, validation; K.D.: writing—reviewing and editing. All authors have read and agreed to the published version of the manuscript.

Funding

This work was supported in part by the National Natural Science Foundation of China under Grant 62273004 and Grant 62403006, in part by the Anhui Provincial Natural Science Foundation of China under Grant 2408085QF184 and Grant 2508085QA035, in part by the Research Fund for Anhui Provincial Talent Innovation Team under Grant 2023AH010011, and in part by the Talent Program of Anhui Province.

Data Availability Statement

Not applicable.

Conflicts of Interest

The authors declare no conflict of interest.

Use of AI and AI-Assisted Technologies

No AI tools were utilized for this paper.

References

1. Qi, W.; Zhang, N.; Park, J.H.; et al. Protocol-based synchronization of semi-Markovian jump neural networks with DoS attacks and application to quadruple-tank process. *IEEE Trans. Autom. Sci. Eng.* **2024**, *22*, 1377–1389.
2. Yao, L.; Huang, X.; Wang, Z.; et al. A multi-sensor-based switching event-triggered mechanism for synchronization control of markovian jump neural networks under DoS attacks. *IEEE Trans. Inf. Forensics Secur.* **2024**, *19*, 7548–7559.
3. Lin, W.J.; Wang, Q.; Tan, G. Asynchronous adaptive event-triggered fault detection for delayed Markov jump neural networks: A delay-variation-dependent approach. *Neural Netw.* **2024**, *171*, 53–60.
4. Chang, X.K.; He, Y. Extended dissipativity analysis for delayed Markovian jump neural networks via a delay-interval-adjustable-based Lyapunov-Krasovskii functional. *IEEE Trans. Cybern.* **2025**, *55*, 3158–3170.
5. Zhang, X.; Luo, B.; Wang, Z.P.; et al. Adaptive boundary control for synchronization of reaction-diffusion neural networks with random time-varying delay. *IEEE Trans. Neural Netw. Learn. Syst.* **2025**, *36*, 14624–14635.
6. Song, X.; Man, J.; Ahn, C.K.; et al. Synchronization in finite/fixed time for Markovian complex-valued nonlinear interconnected neural networks with reaction-diffusion terms. *IEEE Trans. Netw. Sci. Eng.* **2021**, *8*, 3313–3324.
7. Wei, W.; Zhang, B.; Cheng, J.; et al. Time-space sampled-data control for semi-Markov reaction-diffusion neural networks: Adopting multiple event-triggered protocols. *Inf. Sci.* **2025**, *698*, 121779.
8. Zhang, Y.; Wu, Z. Event-based asynchronous H_∞ control for nonhomogeneous Markov jump systems with imperfect transition probabilities. *IEEE Trans. Cybern.* **2024**, *54*, 6269–6280.
9. Yan, H.; Tian, Y.; Li, H.; et al. Input-output finite-time mean square stabilisation of nonlinear semi-Markovian jump systems. *Automatica* **2019**, *104*, 82–89.
10. Ma, Y.; Kong, C. Dissipative asynchronous T-S fuzzy control for singular semi-Markovian jump systems. *IEEE Trans. Cybern.* **2022**, *52*, 5454–5463.
11. Xu, Z.; Su, H.; Shi, P.; et al. Asynchronous H_∞ control of semi-Markov jump linear systems. *Appl. Math. Comput.* **2019**, *349*, 270–280.

12. Shen, H.; Wang, X.; Wang, J.; et al. Robust composite H_∞ synchronization of Markov jump reaction-diffusion neural networks via a disturbance observer-based method. *IEEE Trans. Cybern.* **2022**, *52*, 12712–12721.
13. Qi, W.; Yuan, Z.; Zong, G.; et al. Dynamic-memory protocol-based synchronization for semi-Markov jump reaction-diffusion CDNs. *IEEE Trans. Cybern.* **2025**, *55*, 969–980.
14. Han, X.; Wu, K.; Yuan, X. Observer-based asynchronous boundary stabilization for stochastic Markovian reaction-diffusion neural networks. *IEEE Trans. Cybern.* **2024**, *54*, 6667–6678.
15. Li, H.; Shi, P.; Yao, D. Adaptive sliding-mode control of Markov jump nonlinear systems with actuator faults. *IEEE Trans. Autom. Control* **2017**, *62*, 1933–1939.
16. Tao, J.; Lu, R.; Shi, P.; et al. Dissipativity-based reliable control for fuzzy Markov jump systems with actuator faults. *IEEE Trans. Cybern.* **2017**, *47*, 2377–2388.
17. Pang, Y.; Zhuang, G.; Xia, J.; et al. H_∞ security control for singular jump systems with actuator faults and DoS attacks under switching-like adaptive trigger and application to OCCP. *IEEE Trans. Autom. Sci. Eng.* **2025**, *22*, 7955–7966.
18. Hu, M.; Cheng, J. Asynchronous output feedback control for fuzzy Markov jump systems with actuator faults and deception attacks. *Nonlinear Dyn.* **2024**, *112*, 20035–20045.
19. Hu, M.; Park, J.; Cheng, J. Finite-time asynchronous control for semi-Markov jump systems with random uncertainties and actuator faults. *Inf. Sci.* **2024**, *674*, 120701.
20. Yang, H.; Jiang, Y.; Yin, S. Adaptive fuzzy fault-tolerant control for Markov jump systems with additive and multiplicative actuator faults. *IEEE Trans. Fuzzy Syst.* **2021**, *29*, 772–785.
21. Tabuada, P. Event-triggered real-time scheduling of stabilizing control tasks. *IEEE Trans. Autom. Control* **2007**, *52*, 1680–1685.
22. Girard, A. Dynamic triggering mechanisms for event-triggered control. *IEEE Trans. Autom. Control* **2014**, *60*, 1992–1997.
23. Gu, Z.; Yue, D.; Tian, E. On designing of an adaptive event-triggered communication scheme for nonlinear networked interconnected control systems. *Inf. Sci.* **2018**, *422*, 257–270.
24. Zhang, Q.; Yan, H.; Zhang, H.; et al. H_∞ control of singular system based on stochastic cyber-attacks and dynamic event-triggered mechanism. *IEEE Trans. Syst. Man Cybern. Syst.* **2020**, *51*, 7510–7516.
25. Chen, M.; Wang, Y.; Wang, X. Input-output finite-time guaranteed cost control for time-varying systems based on an aperiodic adaptive event-triggered mechanism. *J. Syst. Sci. Complex.* **2023**, *36*, 1070–1088.
26. Peng, C.; Han, Q.; Yue, D. To transmit or not to transmit: A discrete event-triggered communication scheme for networked Takagi-Sugeno fuzzy systems. *IEEE Trans. Fuzzy Syst.* **2013**, *21*, 164–170.
27. Luo, W.; Chen, H.; Zong, G.; et al. Event-triggered neural asynchronous control of nonhomogeneous Markov jump power systems with hybrid cyber attacks and unknown states. *IEEE Trans. Power Syst.* **2025**, *40*, 3874–3886.